4th International Conference on Water Resources and Arid Environments (ICWRAE 4): 749-756
5-8 December 2010, Riyadh, Saudi Arabia

Real Time Monitoring of Soil Water Infiltration Using Electrical Capacitance Volume-tomography (ECVT)

Muhammad Mukhlisin[1,2], Marlin Ramadhan Baidillah[1], Ahmed El-Shafie[1] and Mohd Raihan Taha[1]

[1]Department of Civil and Structural Engineering, Universiti Kebangsaan Malaysia
[2]Department of Civil Engineering, Polytechnic Negeri Semarang, Indonesia

Abstract: Electrical Capacitance Volume Tomography (ECVT) recently has been developed and used for extensive process imaging research due to its noninvasive nature, capability of differentiating between different components based on permittivity distribution to obtain real time and volumetric (4D) image of the object. This paper is describing the first attempt to apply this prospective technique in soil-water sciences field. The objective of this paper is to monitor by real time imaging of the infiltration of water in the soil. The procedure is as follows: 3 liters volume of soil in the vessel is under artificial a rainfall with debit of water 7.2 ml/s. The 32 channel ECVT sensors installed on a vessel. The infiltration of water can be detected by sensors because it changed capacitance value of a soil medium as has different permittivity value with the soil. As a result of measurement, this laboratory experiment can be identify an infiltration of water in the soil and qualitatively imaged by real time.

Key words: Soil water infiltration • ECVT • Real time imaging

INTRODUCTION

Monitoring water infiltration using small soil column experiment is an important to evaluate water flow and solute transport through unsaturated soil. A better understanding of soil water infiltration process is essential for understanding and predicting of dynamic soil water infiltration and solute transport. However, there are some difficulties with current techniques for monitoring real time 3-dimensional soil water infiltration in unsaturated soil column studies.

To study the underlying physics of water infiltration into the unsaturated soil some methods have been conducted for several years. There are two main ways of study the infiltration of water, by numerical modeling and field monitoring (in-situ experiment). For numerical modeling many study have been conducted (e.g., [1-7] and all have confirmed that rainwater infiltration into a slope has a major effect on slope instability and landslide fluidization. In experiments field monitoring, numerous researcher have applied some techniques to monitor soil water infiltration, such as Time Domain Reflectometry [8], Disc Infiltrometer [9], Microwave Radiometer [10]. Ground penetrating radar [8], Electrical Resistance Tomography [11-13]. Although, these techniques could generates data by temporal resolution but it still limited in 2-Dimension spatial data. Therefore, a monitoring technique which can generates 3-Dimension of spatial data simultaneously is still a challenge in soil-water field.

There is a well-known noninvasive technique that called tomography which has been used in many research area fields (e.g. chemical engineering, geophysics, medicine) because it can generates images of internal structures. The recent progress in development of process tomography has provided in-depth insights into the complex multiphase flow phenomena in many industrial processes [14]. One of the tomography techniques which have a great potential is Electrical Capacitance Volume-Tomography (ECVT).

ECVT is a dynamic volume imaging based on the principle of electrical capacitance tomography (ECT) [14]. This technique is not a post processing 4D image reconstruction because it creates movie images of electrical permittivity directly from multi-frame volumetric data. From engineering point of view, this technique has noninvasive nature, capability of differentiating between different components based on permittivity distribution to obtain real time and volumetric (4D) image of the object [14]. Actually, soil is a mixture of solid, air and water. Because the dielectric constant of water is greater than

Corresponding Author: Muhammad Mukhlisin, Department of Civil and Structural Engineering, Universiti Kebangsaan Malaysia

others, i.e. 81 for frequencies less than 1000 MHz, the value of dielectric for the soil is depends on the water content [14]. This physical property makes ECVT as a great potential tool to monitoring the infiltration of water in soil.

In this study, a small soil column with ECVT system is developed to monitor water infiltration into an unsaturated soil. This study is the first attempt applying ECVT to monitor soil water infiltration by real time 3D imaging.

MATERIALS AND METHOD

Principle of ECVT: In the literature: the permittivity distribution is related to capacitance measurement according to Poisson equation:

$$\nabla \cdot (\varepsilon(x,y,z))\nabla\phi(x,y,z) = -\rho(x,y,z) \quad (1)$$

Where $\varepsilon(x,y,z)$ is permittivity distribution, $\phi(x,y,z)$ is electrical potential distribution and $\rho(x,y,z)$ is charge distribution.

The mutual capacitance between two pairs of electrodes is given by the ratio between stored charge and potential difference as in equation:

$$c_{ij} = \frac{Q_{ij}}{\Delta v_{ij}} \quad (2)$$

Where:

c_{ij} is the mutual capacitance and • $V_{i,j}$ is the potential difference between electrodes I and j respectively and Δv_{ij} is the charge on the receiving electrode. Q_i is found by applying Gauss law:

$$Q_j = \bullet_{\Gamma j} \varepsilon(x,y,z) \bullet \phi(x,y,z) \,.\, \hat{n}\, dl \quad (3)$$

Where:

Γ_j is a closed path enclosing the detecting electrode and $\hat{n}$ is a unit vector normal to Γ_j. Using Eq. (1) and (3), the mutual capacitance is calculated as:

$$C_{i,j} = \frac{1}{\Delta v_{i,j}} \oint_{\Gamma_j} \varepsilon(x,y,z)\nabla\varnothing(x,y,z).\hat{n}dl \quad (4)$$

So, the first problem in ECVT is how to measure the capacitance. This is known as forward problem.

The capacitance value of medium is measured by using differential method. This method considers the unknown capacitance to be an element of an active differentiator [15]. The data acquisition system for this task is made by CTech Labs (Edwar Technology Co.) which is capable of capturing image data up to 496 independent measurements for 0.25 seconds.

Fig. 1: The arrangement design of sensor ECVTg2

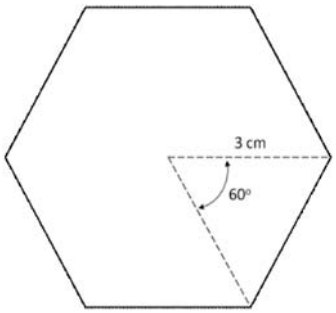

Fig. 2: Sensor dimension

Performing volumetric image, ECVT required multiple electrodes that arranged in the boundary of the region. The number of independent measurement is depended on the number of electrodes as described with this equation:

$$M = ne \,.\, (ne\text{-}1)\,/2 \quad (5)$$

Where:

ne is the number of electrode. Due to the soft field of the electrical field, the capacitance measurement that generates simultaneous information of the volumetric properties can be made using arbitrary shapes of sensors and vessels [16] Based on Eq. (4), the measured capacitance is depending on the area enclosing the detector electrode. Therefore, the sensitivity of sensor to differentiate the change of permittivity value is depending on the sensor design. The choice of geometry sensors is based on the most optimum geometry to transfer electrical field. We choose hexagonal sensors that arranged as showed in Fig. 1 and the dimension of a sensor as depicted in Fig. 2.

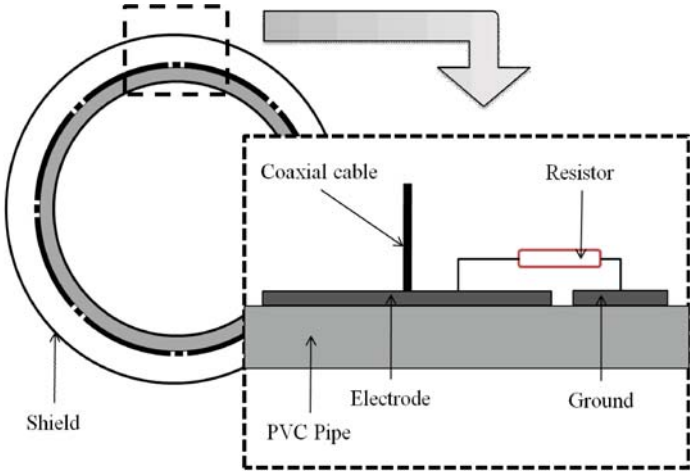

Fig. 3: ECVT sensor in detail pattern

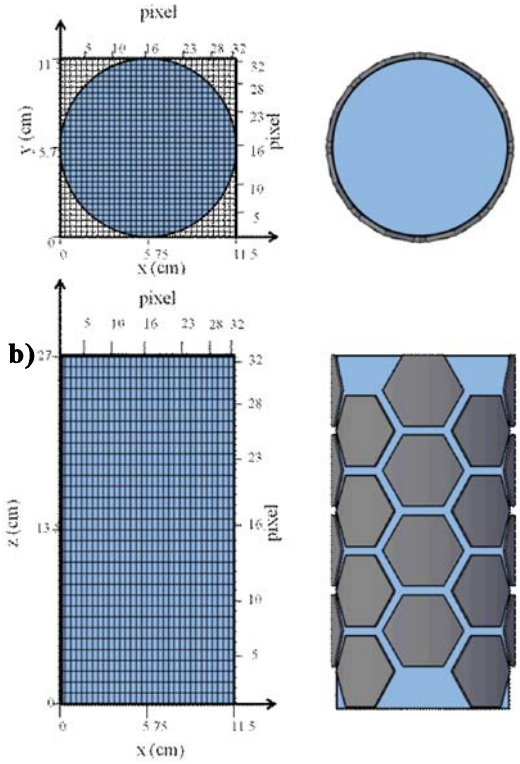

Fig. 4: a) Top view b) Front view

In detail pattern, the components of a sensor simplify as described in Fig. 3. The material for the components that used as electrode and ground is composed from copper. The electrode then linked to coaxial cable that used to transfer the measured voltage between electrode and ground to the Data Acquisition System.

Estimating the permittivity distribution from the measured capacitance data is known as Inverse Problem. In this step we used the sensitivity model to solve the inverse problem. The sensitivity model is a linearization method that inspired by hard field tomography. Using the linearization technique, the domain of the system is divided into a number of pixels (see Fig. 4) and assumed that permittivity distribution is independent with electric fields distribution. The linearization form of Eq. (4) is written in matrix expression as.

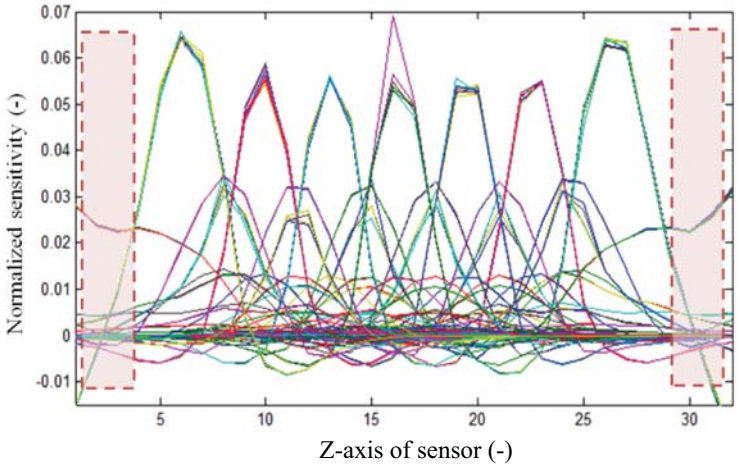

Fig. 5: Sensitivity matrix curve for hexagonal sensor. Dead zone area is indicated in dashed line area

$$C = SG \tag{6}$$

Where:

C is a M-dimension capacitance data vector, G is a N-dimension image vector and S is a M x N dimension sensitivity matrix. M is the number of electrode-pair combinations (see Eq.(5)). N is the number of voxel.

$$N = nx \times ny \times nz \tag{7}$$

Where:

nx, ny, nz are the numbers of voxel at x, y, z axis respectively. Using a back projection technique, the image vector can be estimated by

$$G = S^T C \tag{8}$$

The sensitivity matrix S is depending on the geometry of the sensor. Therefore, S is the unique property of sensor to capable differentiating the change of permittivity distribution. The axial distribution of normalized sensitivity for 496 capacitance pairs is depicted in Fig. 5. The convergence of the iterative reconstruction process is determined by the variation where the difference in the maximum and minimum values in one level and the smoothness of the slope of the sensitivity distribution curves along the axial direction [16]. In Fig.5, there are many variations in the axial direction. Therefore, an object in almost all regions in this sensor will be differentiated. Only in bottom and upper layer that no much variations. Therefore in these layers are found a dead zone. In dead zone area, the image reconstructed is a relative difficult to converge.

Before the experiment is conducted, the first step is performing calibration process. The purpose of this step is to normalize the capacitance data so that the value is ranged between 0 and 1, as described in Eq. (9). This first step is important in tomography science because the quality image resulted will depend strongly on successfully calibration process.

In this step, low-permittivity medium ε_l is defined to 0 in range scale color and high-permittivity medium ε_h is defined to 1 in range scale color. The normalized capacitance is expressed by

$$C_{i,j} = \frac{cm(i,j) - C_l(i,j)}{Ch(i,j) - C_l(i,j)} \tag{9}$$

($I = 1 \ldots ne, j = i + 1 \ldots ne$) where $C_{i,j}$ is the normalized capacitance of electrode pair I-j, $C_m(i,j)$ is the measured capacitance of electrode pair I-j and $C_l(i,j)$, C_h (i,j) are the capacitances of electrode with the function of ε_l and ε_h, respectively. The image is reconstructed on 32x32x32 resolution based on Iterative Linear Back Propagation (ILBP). The relationship size between pixels and real size in a vessel is can be seen in Fig. 4. The lengths for a pixel nx, ny, nz are 0.358 cm, 0.358 cm and 0.84 cm, respectively. Therefore the volume for a voxel is 0.11 cm^3.

Experimental Set-up of Ecvt System: Figure 6 shows the experiment set-up. The experiment was conducted in a vertical column vessel. The column is 11.5 cm diameters, 27 cm height and 3 liters volume. ECVT sensors is attached in periphery of a vertical column and composed into 32 electrodes distributed in four planes. All sensors connected to data acquisition system and then the data is sent to the PC to be reconstructed.

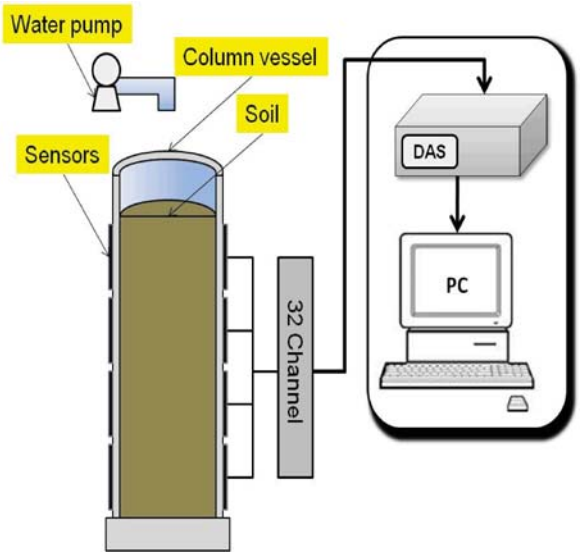

Fig. 6: Sketch of an ECVT system

In this study 2 cases experiments were conducted. The fist experiment was done with supplying water into the empty vessel, while in the second experiment the vessel was filled with soil then artificial rain water was supplied to the soil. For testing the image reconstruction performance of ECVT in capability detecting the change of water, experiment 1 is then conducted first. In this experiment, the empty column that air as background medium is filled water. The water volume is increased by supply water discharge 6 ml/s. In this experiment air and water are as low-permittivity medium ε_l and high-permittivity medium ε_h, respectively.

For the second experiment, 3 liters volume of soil in the vessel is under artificial rainfall with discharge of water 7.2 ml/s. During a water supply, the data capacitances is measured iteratively and sent to the computer. Frequency of data acquisition is made to 1 frame per second. In this experiment, dry soil and water are as low-permittivity medium ε_l and high-permittivity medium ε_h, respectively.

Soil Properties: The soil material used in this study is sand where the soil (sand material) was collected from Cisadane river, Tangerang, Indonesia. The soil contains finer than 0.075 mm is 0.8%. The specific gravity, density and water saturation of soil are 2.663, 1.55 g cm-3 and 15.00 %, respectively. While from grain size distribution of the soil comprises of 83 % of medium sand and 17 % of fine sand.

RESULTS AND DISCUSSION

Imaging of 3d Water Flow in the Vessel: Figure 7 and 9 shows the reconstructed data that using ILBP (Iterative Linear Back Propagation) as image reconstruction algorithm and took 10 iterations to inversed the data. From the first experiment can be seen the behavior of the ECVT system when the medium is filled by water continuously. Figure 7 showed the background medium that air was filled by water flow. The increasing of water content in the vessel can be seen by increasing of red color in the medium. The figure shows that the water fill up to a half of vessel at 300 s and the water almost full the vessel at 500 s. Reconstruction image of increasing of water flow in the vessel can be illustrated very well second by second in this study.

Figures 7 (a-l) are representative of normalized capacitance from 12 different frames. In each frame content simultaneous 496 measurements can be estimated for one second acquisition. While Fig. 8 shows normalized mean capacitance value for the all number data of measurements for each frame, where value 0 and 1 illustrated empty and full water in the vessel, respectively. Increasing of water in the vessel resulted an increasing of the normalized mean capacitance value as well. From this figure can be seen that the value of mean normalized capacitance per frame start to increase at around 100 s and simultaneously increase until at around 500 s. The value of mean normalized capacitance fixed in level 1 from 500s to 600s, which mean the water was full in the vessel (see Figs. 7 and 8).

Imaging of 3d Soil Water Infiltration: Figure 9 shows images of soil water infiltration in eight different times. The color bar scale from 0 to 1 is indicated the value of normalized permittivity. The blue color is means that the medium is fully low-permittivity medium (i.e. dry soil) and the red one is full of high-permittivity medium (i.e. saturated soil water content). The figure illustrated the pattern soil water infiltration in the vessel. Although water supply from the top of central point of the vessel, the water tend to infiltrated to soil from the edge of the vessel, then soil water infiltration up to the half of the vessel at around 350s. Until the end of experiment some part of blue color are showed in bottom part of the vessel. This is due to air trap that caused the water infiltration cannot reach this area.

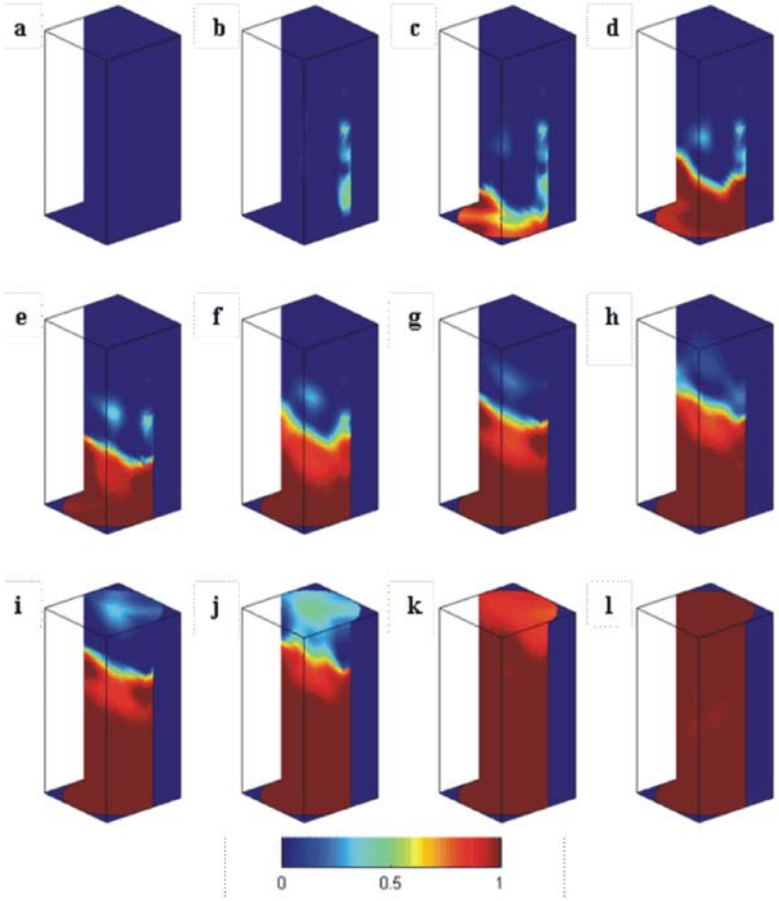

Fig. 7: Permittivity distribution of water at time (a) 1 s, (b) 50 s, (c)100 s, (d)150 s, (e)200 s, (f) 250 s, (g)300 s, (h)350 s, (i)400 s, (j)450 s, (k)500 s, (l)550 s.

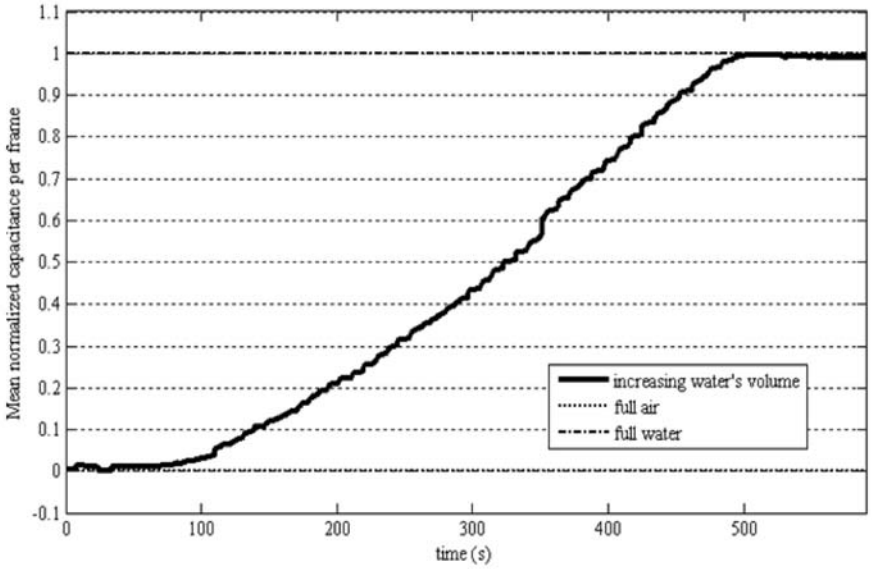

Fig. 8: Mean-normalized capacitance per frame for air-water calibration

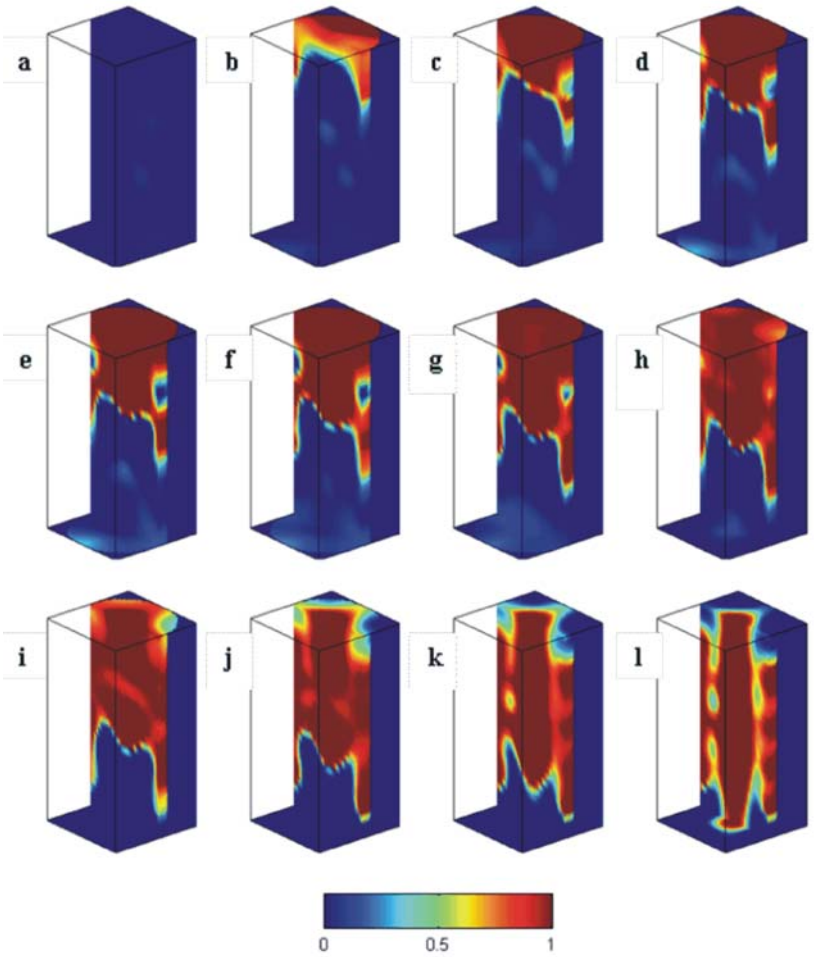

Fig. 9: Permittivity distribution of soil water infiltration at time (a)1 s, (b)50 s,

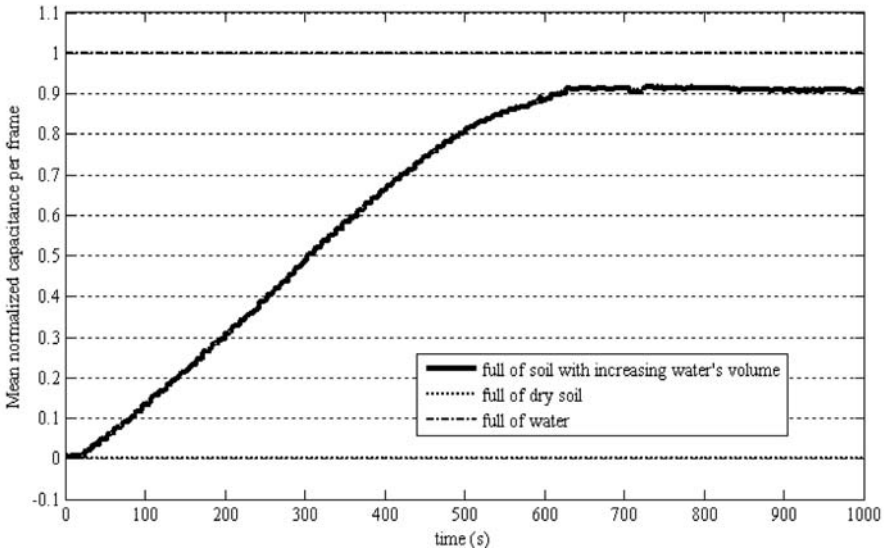

Fig. 10: Mean-normalized capacitance per frame for dry soil-water calibration

The capacitance's value of a medium is dependent with the permittivity value. Therefore, different medium made the color distribution will be different too. Increasing of water infiltration in the soil made changed of the soil permittivity. The changing of soil permittivity value makes the capacitance and then so do the color image are changed.

Figure 10 shows mean-normalized capacitance for 1000 frame. This figure shows that the value of mean-normalized capacitance in the system is 0 for dry soil condition, while for saturated soil the value is around 0.9. Increasing of water infiltration in the soil resulted the increasing of mean-normalized capacitance. When the soil is saturated, the permittivity will not as high as pure water. Therefore, the value of mean-normalized capacitance and the color bar in figure 9 and 10 will not reach the pure water value.

CONCLUSION

The monitoring of water flow and soil water infiltration in unsaturated soil has been conducted in this study. The system has successfully reconstructed the image in real time 3D of water flow and soil water infiltration in the vessel. The real time of increasing of water level in the vessel can be monitor perfectly. In additional this study has also successfully monitor water infiltration in unsaturated soil. Both of experiment can be entirely monitored due to the system can determine the differences of the normalized dielectric permittivity distribution between water and saturated soil which is 1.0 and around 0.9, respectively. The system has also successful in real time 3D imaging the concentration of moisture soil water content as showed in the range of scale color. This study shows that ECVT is a very potential method for real time monitoring process in soil-water sciences field.

REFERENCES

1. Tsaparas, I., H. Rahardjo, D.G. Toll.and E.C. Leong, 2002. Controlling parameters for rainfall-induced landslides. Computers and Geotechnics. 29: 1-27.
2. Cho, S.E. and S.R. Lee, 2001. Instability of unsaturated soil slopes due to infiltration. Computers and Geotechnics. 28: 185-208.
3. Gasmo, J.M., H. Rahardjo and E.C. Leong, 2000. Infiltration effets on stability of a residual soil slope. Computers and Geotechnics. 26: 145-165.
4. Shakya, N.M. and S. Chander, 1998. Modelling of hillslope runoff processes. Environmental Geol., 35: 115-123.
5. Wilkinson, P.L., M.G. Anderson and D.M. Lloyd, 2002. An Integrated hydrological model for rain-induced landslide prediction. Earth Surface Processes and Landforms. 27: 1285-1297.
6. Mukhlisin, M., K. Kosugi, Y. Satofuka and T. Mizuyama, 2006. Effects of Soil Porosity on Slope Stability and Debris Flow Runout at a Weathered Granitic Hillslope. Vadoze Zone J., 5: 283-295.
7. Mukhlisin, M., M.R. Taha. and K. Kosugi, 2008, Numerical analysis of effective soil porosity and soil thickness effects on slope stability at a hillslope of weathered granitic soil formation, Geosciences J., 12(4): 401-410.
8. Huisman, J., C. Sperl, W. Bouten. and J. Verstraten, 2001. Soil water content measurements at different scales: accuracy of time domain reflectometry and ground-penetrating radar. 48-58
9. Moret, D. and C. Gonzalez, 2009. New method for monitoring soil water infiltration rates Applied to a Disc Infiltrome., 315-322.
10. Jackson, T.J., T.J. Schmugge. and W.J. Rawls, 1998. Soil Water Infiltration Observation with Microwave Radiometers. IEEE, 36(5): 1376-1383.
11. Brunet, P., R. Clement. and C. Bouvier, 2010. Monitoring soil water content and deficit using Electrical Resistivity Tomography (ERT)-A case study in the Cevennes area, France. 146-153.
12. Batlle-Aguilar. J., M. Pessel, P. Tucholka, Y. Coquet. and P. Vachier, 2009. Axisymetrical Infiltration in Soil Imaged by Noninvasive Electrical Resistivimetry. Soil Sci. Soc. Am. J., 73: 510-520.
13. Koestel. J., R. Kasteel, A. Kemna, O. Esser, M. Javaux., A. Binley. and H. Vereecken, 2009. Imaging Brilliant Blue Stained Soil by Means of Electrical Resistivity Tomography. Vadose. Zone. J., 8: 963-975.
14. Warsito, W., Q. Marashdeh. and L. Fan, 2007a. Real Time Volumetric Imaging of Multiphase Flows Using Electrical Capacitance Volume-Tomography (ECVT). *5th World Congress on Industrial Process Tomography*.
15. Harteveld, W.K., P.A. Van Halderen, R.F. Mudde, C.M. Van Den Bleek, H.E.A. Van Den Akker and B. Scarlett, 1999. A fast active differentiator capacitance transducer for electrical capacitance tomography. 1st Word Congress on Industrial Process Tomography, Buxton, Greater, Manchester, April, 14-17: 564-567.
16. Warsito, W., Q. Marashdeh and L.S. Fan, 2007. Electrical Capacitance Volume Tomography. IEEE , 7(4): 525-535.